ELSEVIER

Tectonophysics 359 (2002) 65–79

TECTONOPHYSICS

www.elsevier.com/locate/tecto

Ultra-low frequency electromagnetic measurements associated with the 1998 M_w 5.1 San Juan Bautista, California earthquake and implications for mechanisms of electromagnetic earthquake precursors

D. Karakelian *, S.L. Klemperer, A.C. Fraser-Smith, G.A. Thompson

Department of Geophysics, Stanford University, Stanford, CA 94305-2215, USA

Received 6 December 2001; accepted 16 August 2002

Abstract

Ultra-low frequency (ULF: 0.01–10 Hz) magnetic field anomalies prior to $M \geq 6.0$ earthquakes have been reported in various regions of the world. Here, we test whether smaller magnitude earthquakes have associated ULF anomalies by using continuous measurements made ~9 km above and ~2 km NE of the epicenter of the M_w 5.1 8/12/98 San Juan Bautista, CA earthquake. Half-hour spectral averages of the magnetic field data in nine different ULF frequency bands show no long-term (days to weeks) magnetic field anomaly prior to the earthquake. In addition, magnetic and electric field polarization shows no anomalous behavior clearly associated with seismic activity. An ~0.02 nT increase in activity for 2 h prior to the earthquake is close to the background noise levels precluding identification of a precursor. We present scaling calculations to show if precursory ULF anomalies are related to the size of the earthquake. The observed ~0.02 nT increase is the approximately expected magnetic anomaly prior to the San Juan Bautista (SBJ) earthquake, based on the anomaly observed prior to the 1989 Loma Prieta (LP) earthquake. Our reexamination of previously proposed dilatant-conductive and piezomagnetic mechanisms for ULF precursors shows that these effects are consistent with the observations prior to the SJB earthquake based on the observations (i.e., lack of a strong precursor). In contrast, previously proposed electrokinetic and magnetohydrodynamic (MHD) mechanisms do not appear to be appropriate for this particular earthquake. This analysis further supports the hypothesis that precursory ULF signals are related to the size of the earthquake.

Keywords: San Juan Bautista earthquake; Earthquake precursors; Electromagnetic-earthquake precursors; ULF signals; Magnetic field anomalies; Co-seismic signals

1. Introduction

Ultra-low frequency (ULF: 0.01–10 Hz) anomalies in the magnetic and electric fields prior to several $M \geq 6.0$ earthquakes have been reported in various, geologically distinct regions of the world. In partic-

* Corresponding author. Tel.: +1-650-725-0278; fax: +1-650-725-7344.

E-mail address: darcy@pangea.stanford.edu (D. Karakelian).

0040-1951/02/$ - see front matter © 2002 Elsevier Science B.V. All rights reserved.
PII: S0040-1951(02)00439-0

ular, Fraser-Smith et al. (1990) recorded anomalous magnetic field fluctuations prior to the October 17, 1989 Loma Prieta $M_s = 7.1$ earthquake in central California (Fig. 1), which included an increase in activity about 2 weeks prior to the main shock that continued until an even larger amplitude increase started 3 h before the main shock. Multiple, but not mutually exclusive, possible physical explanations have been proposed (Draganov et al., 1991; Gershenzon and Gokhberg, 1994; Fenoglio et al., 1995; Merzer and Klemperer, 1997). Other anomalous ULF signals possibly related to earthquakes were recorded several hours prior to the December 7, 1988 $M_s = 6.9$ Spitak, Armenia earthquake (Molchanov et al., 1992; Kopytenko et al., 1993), and both about 2 weeks and a few days before the August 8, 1993 $M_s = 8.0$ Guam earthquake (Hayakawa et al., 1996). In addition to these observations, the ULF band is worthy of attention because these are the highest frequency signals that can reach the Earth's surface with little attenuation if they are generated at typical California earthquake nucleation depths (~ 10 km).

There are fewer reports of ULF anomalies associated with smaller magnitude earthquakes ($M \cong 5$) and aftershocks of major earthquakes (Fenoglio et al.,1993; Park et al.,1993; Villante et al., 2001; Zlotnicki et al., 2001; Karakelian et al., in press; Kopytenko et al., submitted for publication). Although Gershenzon and Bambakidis (2001) show that the sources of most precursory electromagnetic anomalies should be relatively close to the detector, it is unclear whether there is a threshold earthquake magnitude above which ULF anomalies may be produced or whether their detection is directly dependent on the magnitude of the earthquake and distance from the source to the sensor. Molchanov (personal communication) suggests that the size (or possibility of observation) of ULF anomalies may scale with the ratio of earthquake magnitude to sensor distance; yet field evidence for this relationship, which may provide further insight into the mechanism producing precursory ULF activity, is lacking. We show that if ULF anomalies are associated with $M \cong 5$ earthquakes, detection of these anomalies would require surface measurement systems to be very close to the epicenter of the earthquake.

An M_w 5.1 earthquake occurred at 1410 UTC on August 12, 1998 on the San Andreas Fault in central California about 2 km southwest of and 9 km below the Hollister, CA, ULF/seismic station SAO, and thereby provided us with the opportunity to test the hypothesis that ULF anomalies are associated with smaller earthquakes. The earthquake was located 12 km south–southeast of San Juan Bautista at 36.7533°N, 121.4618°W and a depth of 9.2 km (Uhrhammer et al., 1999) (Fig. 2), in the northern creeping-to-locked transition zone of the San Andreas Fault approximately 50 km southeast of the epicenter of the M_s 7.1 Loma Prieta earthquake. SAO is one of the 10 permanent electromagnetic ULF monitoring stations established along the San Andreas Fault (Fig. 2), and is operated and maintained by Dr. H.F. Morrison and colleagues at the University of

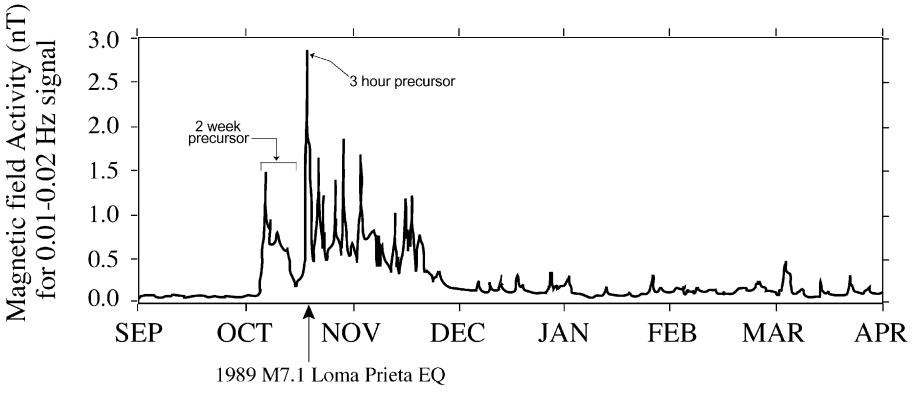

Fig. 1. Magnetic field activity in units of nanoteslas (nT) from September 1989 through April 1990 measured at Corralitos (COR, see Fig. 2), California. The $M = 7.1$ Loma Prieta earthquake occurred on October 17, 1989. (After Fenoglio et al., 1993.)

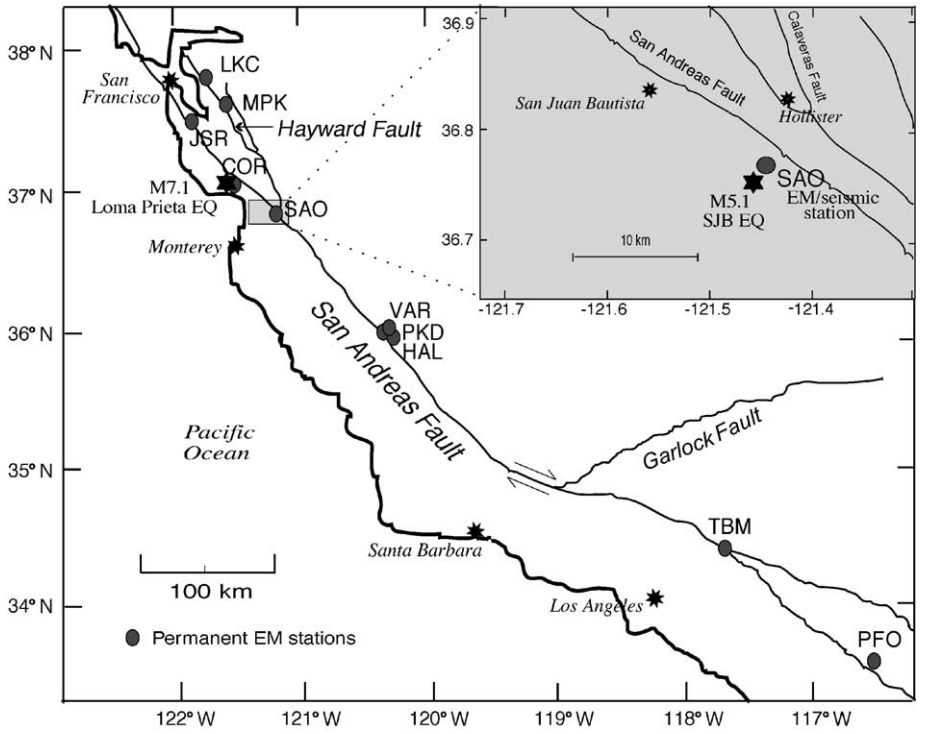

Fig. 2. Map showing permanent ULF stations in California. SAO and PKD are operated by the University of California, Berkeley. All other stations are operated by Stanford University. Inset is a detailed map of the study area showing the location of the $M = 5.1$ SJB earthquake with respect to the ULF station SAO.

California at Berkeley. At the time of the San Juan Bautista (SJB) earthquake, SAO was fully operational and continuously recording magnetic, electric field, and seismic activity, providing a uniquely complete set of ULF and seismic data from a location very close to an earthquake of moderate magnitude.

In this paper, we present both the magnetic and electric field data recorded around the time of the San Juan Bautista earthquake. In addition, we use our results to help constrain the relationship between a precursory ULF signal and earthquake size, a relationship that may provide insight into the mechanisms that produce such anomalous EM fields surrounding earthquakes.

2. Observations

The SAO ULF station (36.765°N, 121.445°W) is equipped with three-component magnetic field induction coils (0.0001–20 Hz) (manufactured by Electromagnetics Instruments (EMI), Richmond, CA, USA) oriented in the geographic east–west, north–south, and vertical directions, and multiple component electric field sensors (DC-20 Hz) utilizing independent $Pb-PbCl_2$ electrodes. These instruments are collocated with a Berkeley Digital Seismic Network (BDSN) site and utilize the 24-bit Quanterra datalogger and the continuous telemetry connection of the BDSN equipment. The EM field data are recorded at 40 samples per second, and the waveform data are archived by the Northern California Earthquake Data Center (NCEDC). Further information about the installation, equipment, and noise levels of typical broadband seismic and ULF stations of this sort are detailed by Uhrhammer et al. (1998) and Karakelian et al. (2000).

Fig. 3 shows the co-seismic response recorded at the time of the SJB earthquake. Co-seismic ULF signals exist on all components of the magnetic and

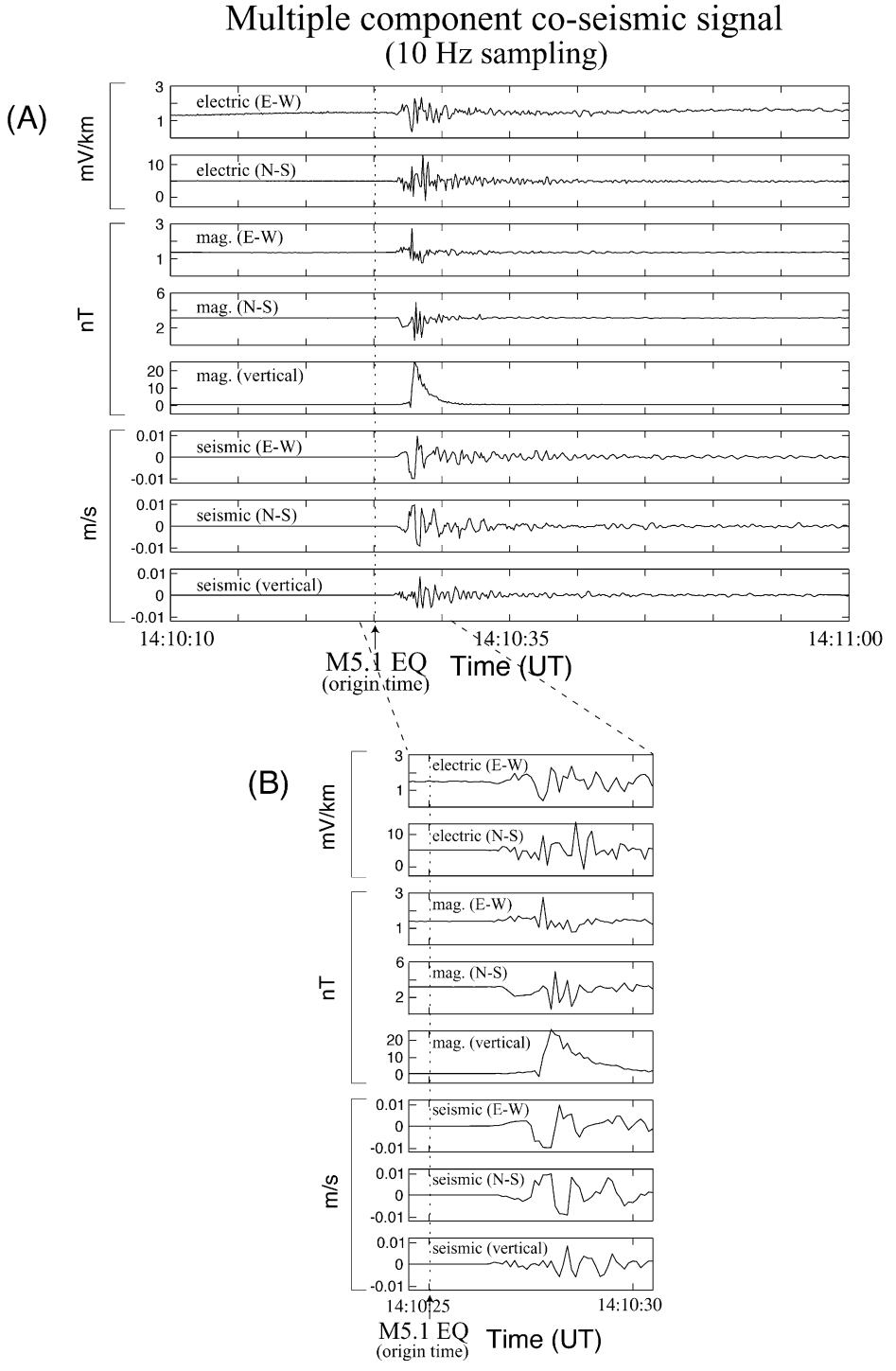
Multiple component co-seismic signal
(10 Hz sampling)
(A)
mV/km
nT
m/s
electric (E-W)
electric (N-S)
mag. (E-W)
mag. (N-S)
mag. (vertical)
seismic (E-W)
seismic (N-S)
seismic (vertical)
3
1
10
0
6
2
20
0.01
-0.01
14:10:10
14:10:35
14:11:00
M5.1 EQ
(origin time)
Time (UT)
(B)
14:10:25
14:10:30

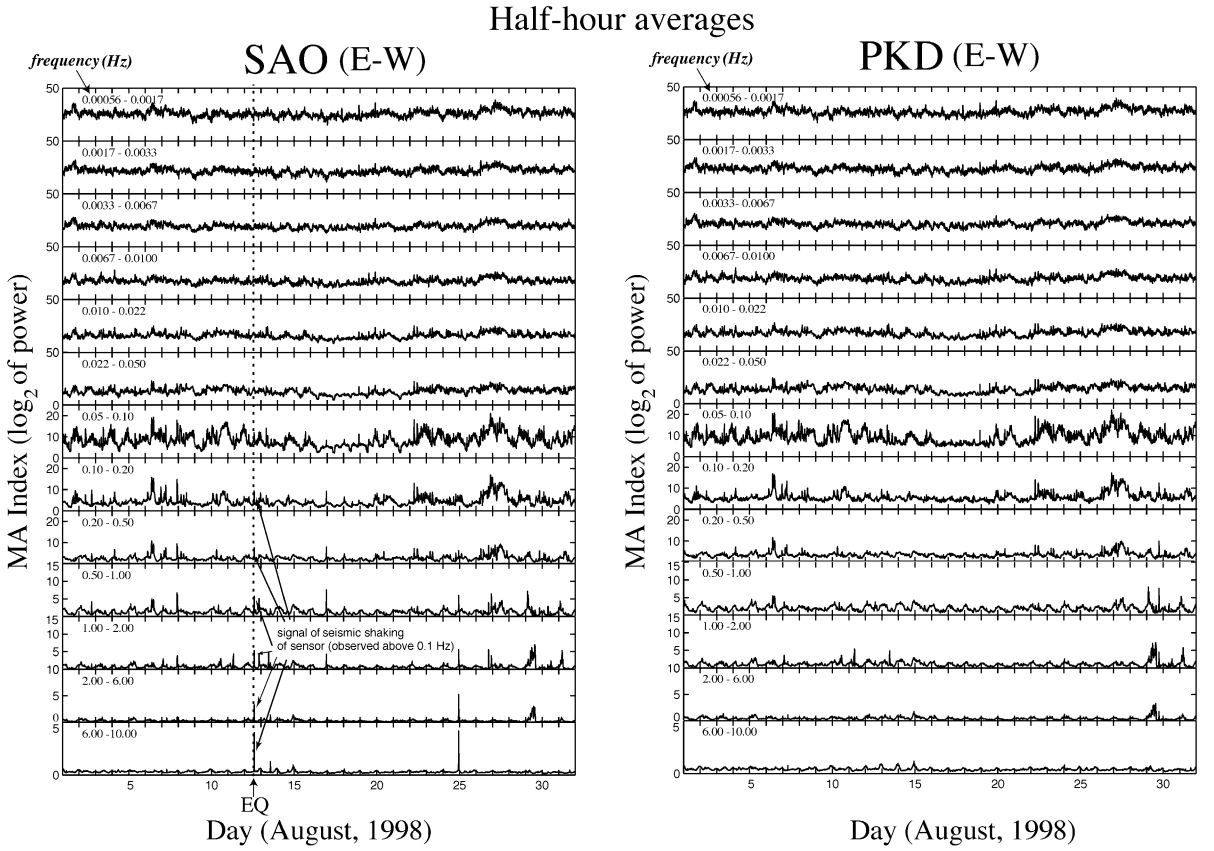

Fig. 4. MA Indices for the E–W magnetic field component for the month of August at SAO and a remote station PKD. MA indices are a set of logarithms to the base two of the halfhourly averages of the power in 13 frequency bands covering the overall range from 0.01 to 10 Hz (data courtesy of the Northern California Earthquake Data Center and the Seismological Laboratory at UC Berkeley). The occurrence time of the SJB earthquake is indicated in the SAO record.

electric fields, and they begin with the arrival of seismic waves at ~14:10:27 (Fig. 3). These results are consistent with those of Nagao et al. (2000) and Karakelian et al. (in press) who conclude that co-seismic signals are not produced at the earthquake source, but rather are due to local effects of passing seismic waves. The visible co-seismic signal records the motion of the sensors in the earth's magnetic field (the same motion as the adjacent seismometer) (e.g., Bernardi et al., 1991) and also perhaps an electro-seismic component due to charge-separation induced by passage of the seismic waves through saturated or partially saturated near-surface strata adjacent to the sensors (Haartsen and Pride, 1997). (Note that the co-seismic response of the vertical magnetic field coil in Fig. 3 has a low frequency component that is likely due to the equipment response.) In this paper, we will focus on observations made prior to this co-seismic signal or minutes after this co-seismic signal in order to differentiate signals of possible tectonic origin from signals produced by ground motion.

Fig. 4 shows east–west component magnetic field data recorded at SAO during August 1998, and the same 31 days of data recorded at a remote reference

Fig. 3. (A) Multiple component co-seismic signal recorded at SAO. Fifty seconds of 10 Hz data are shown (note: scaling varies). The origin time of the $M=5.1$ SJB earthquake that occurred ~9 km below station SAO is indicated. (B) Close up (3× magnification) of co-seismic signal shown in (A). Five seconds of 10-Hz data are shown after the origin time of the SJB earthquake.

site PKD located in Parkfield, CA, approximate distance of 130 km (see Fig. 2). Halfhourly power spectrum averages (MA indices) (Bernardi et al., 1989) in 13 different frequency bands (each about one octave) covering the range 0.00056–10 Hz were calculated to show the variation of magnetic field activity before and after the 8/12/98 earthquake. Comparison of SAO data with the PKD data shows that the predominant component of the magnetic fluctuations evident in these records represents natural geomagnetic variations generated in the upper atmosphere and above. The two MA index records are nearly identical and any local signals, either cultural or tectonic in origin, are largely concealed in this natural activity. A spike in the higher frequency SAO data at the time of the earthquake is due to ground motion causing movement of the magnetic field sensor through the Earth's magnetic field (see Fig. 3).

Since the magnetic indices shown in Fig. 4 are half-hour averages, which have the potential to mask small short-term changes, we next present original magnetic and electric field measurements several hours prior to the earthquake. Fig. 5 shows 1-min averages of the absolute value of the data in the 0.01–0.02 Hz frequency band about 6 h prior to the earthquake. These data show an increase in activity on all components beginning about 2.5 h prior to the main shock. The increase in magnetic field activity is more pronounced on the horizontal components than on the vertical component compared to the normal background noise level of 0.01–0.02 nT, and is also much more pronounced below 0.02 Hz than at higher

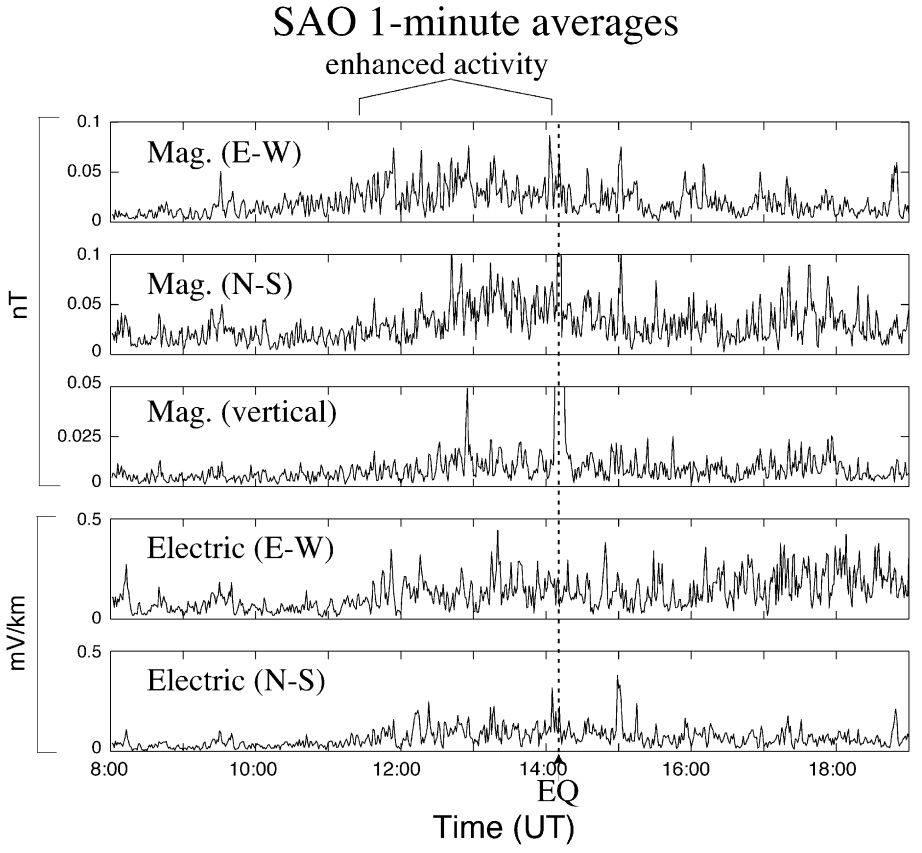

Fig. 5. Multiple component ULF activity at 0.01–0.02 Hz recorded at SAO. Data are 1-min averages of the absolute value of magnetic and electric field amplitudes. The occurrence time of the SJB earthquake is indicated. Shaking of the instruments due to passage of the seismic wave occurs within seconds of the earthquake occurrence.

frequencies (not shown). Both observations are those anticipated for a source at the hypocentral depth of 9 km: the horizontal-component sensitivity probably reflects the higher sensitivity of the horizontal components to low-frequency ionospheric disturbances (Karakelian et al., 2000), whereas the frequency sensitivity can be explained by the "skin depth effect" in which higher frequencies traveling through the Earth are attenuated more than lower frequencies (e.g., Telford et al., 1990). The increase in ULF activity in Fig. 5 also peaks at the time of the earthquake and then returns back to normal background level about 4–5 h later on all components (excluding the east–west component of the electric field on which ULF activity remains elevated). Consequently, it could be related to the upcoming seismic event, even though the amplitude of the increase is comparable to increases due to random noise observed in the data at other times (see Fig. 6).

Fig. 6 shows a similar increase in magnetic field activity a few hours prior to the earthquake at the remote station PKD (~ 120 km distance SE), indicating that this increase may be due, at least in part, to natural atmospheric activity. However, no comparable increase is observed in the ULF data collected at JSR which is slightly closer (~ 100 km distance NW) (Fig. 2). There is a small increase, however, even in the subtracted data (Fig. 6C) that may be an indication

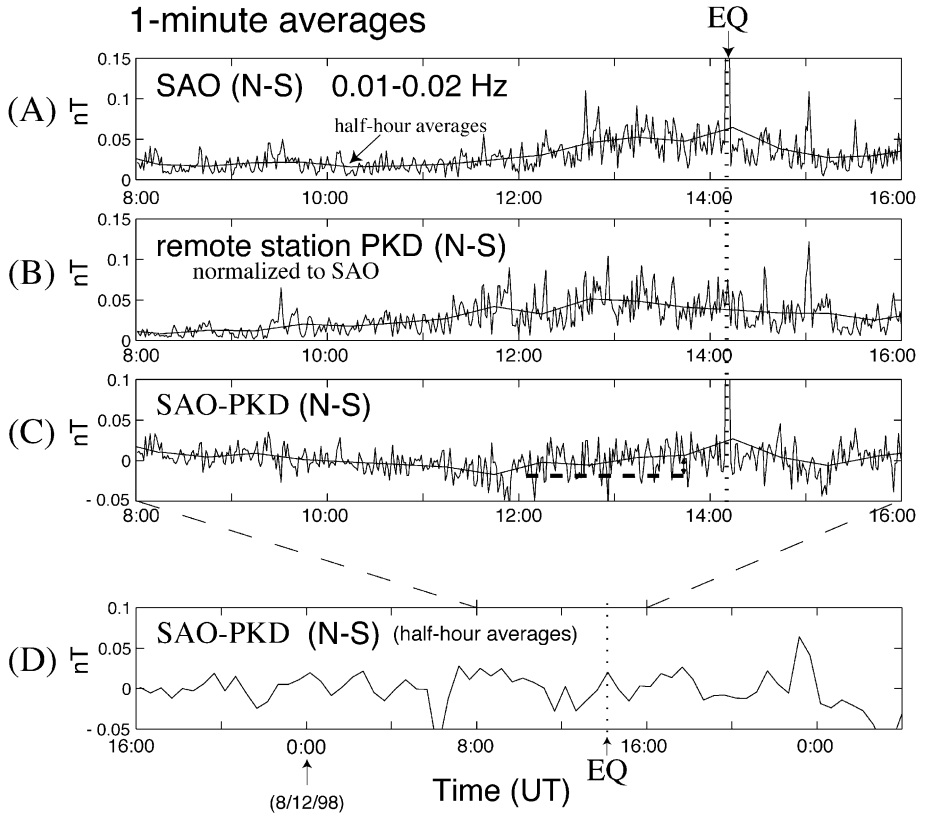

Fig. 6. Magnetic field data recorded on the N–S magnetic field component at both SAO and a remote station PKD. Data in panels (A), (B), and (C) are 1-min averages of the absolute value of the magnetic field amplitude at 0.01–0.02 Hz. PKD data are normalized to SAO by multiplying by $\text{mean}_{SAO}/\text{mean}_{PKD}$ (means were calculated over the 8-h interval shown). Overlaid in a solid line are half-hour averages to show overall trend in data. Dashed line in panel (C) shows the increase in the differenced data. Panel (D) shows half-hour averages of differenced magnetic field data for over 36 h. Diurnal variations in the averages in panel (D) were removed by high-pass filtering frequencies shorter than 12 h. The occurrence time of the SJB earthquake is indicated.

of local activity at SAO, although the increase is small compared to the background noise level at SAO. In addition, Fig. 6D shows that similar increases in the subtracted data at other times are common. We conclude that one cannot state whether or not a precursor occurred, but that any precursor was less than 0.025 nT in the 0.01–0.02 Hz range.

Finally, we analyzed long-term changes in raw electric and magnetic field data. Electric field data may be sensitive to a longer-term change in the resistivity structure of the fault zone, possibly due to an earthquake preparation process in which preexisting conductive pathways in the fault zone are gradually cut off or new conductive pathways around the

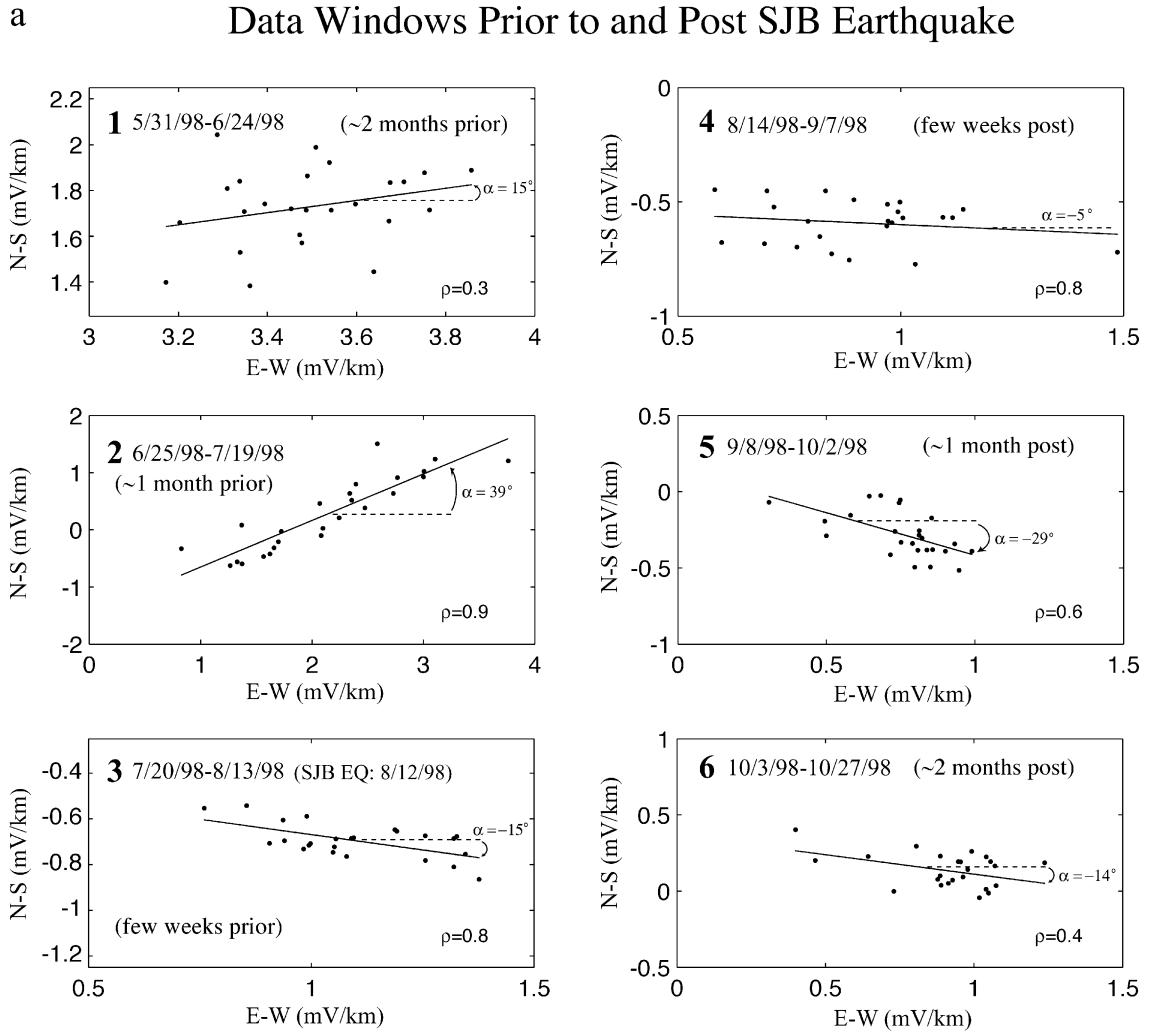

Fig. 7. (a) Electric field polarization plots (N–S vs. E–W component) for six consecutive 25-day periods from May 31 to October 27, 1998. Electric-field data were recorded at 40 Hz, low-pass filtered to 20 Hz and decimated to 20 sps. Noisy spikes in the data were manually removed and the daily averages of the data are plotted in mV/km. Lines derived from least-squares fits to the data as well as correlation coefficients, ρ, are shown for each 25-day period. The direction (α) of the overall trend in the data from an E–W direction is also shown. The SJB earthquake occurred on August 12, 1998, toward the end of the 25-day period shown in plot 3. (b) Electric-field polarization plots similar to those shown in (a) but for time periods 1 year earlier (May 31–October 27, 1997). No $M \geq 4.5$ earthquakes occurred within 50 km of SAO during this time.

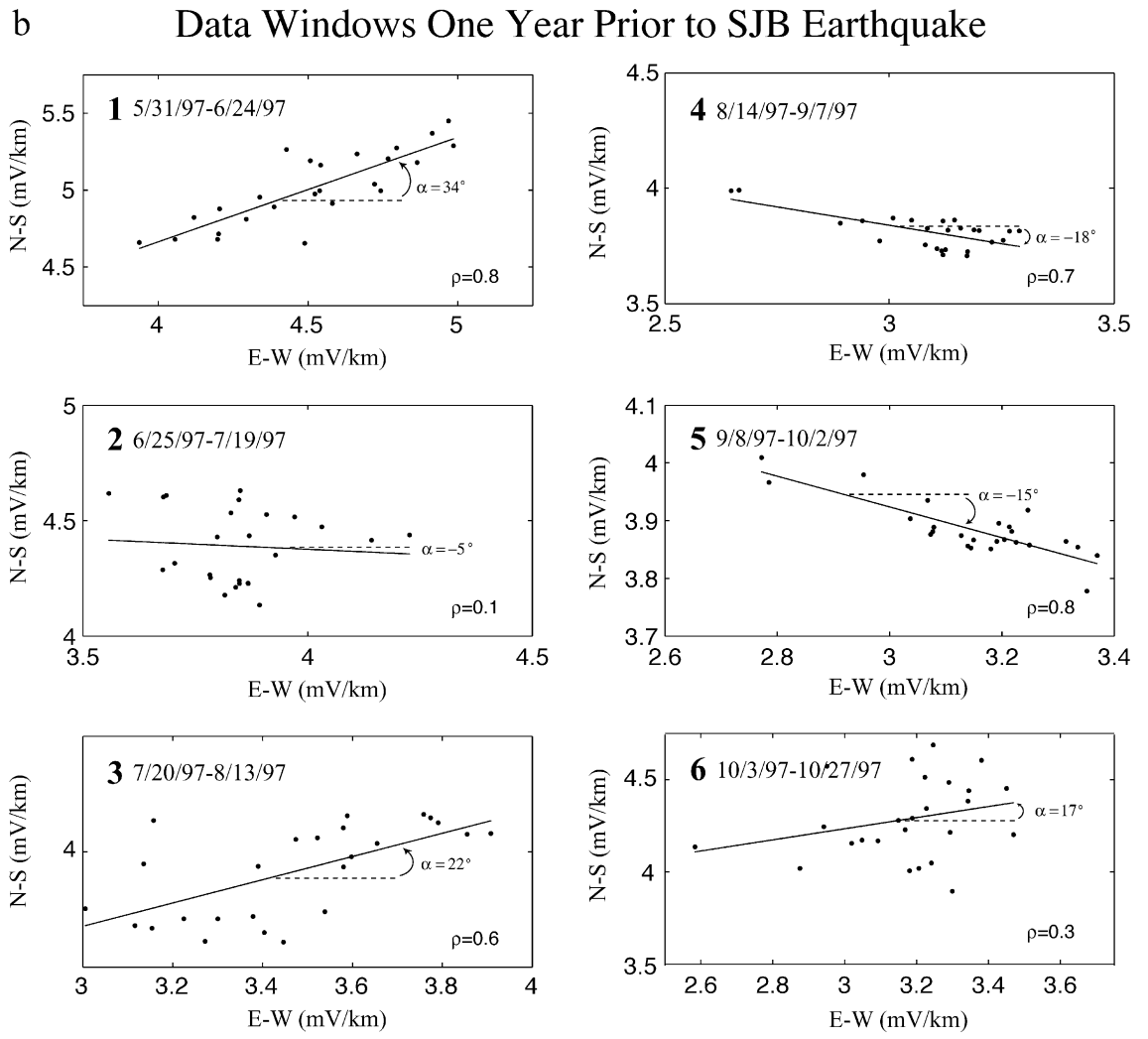

Fig. 7 (*continued*).

fault are formed. Speculatively, a redirection of fluid flow around the fault zone or an increase in fluid flow around the fault zone could result. In addition, geodetic evidence for pore fluid flow (Peltzer et al., 1996) and seismic evidence for pore fluid triggering of aftershocks (Zanzerkia and Beroza, 2001) suggest that pore fluids are present and play an important role in the earthquake process. Despite large scatter at times, the daily averages of the raw electric field data recorded at SAO for 150 days surrounding the SJB earthquake show a change in the dominant direction of electric fields that occurs in the 25-day period prior to the earthquake (Fig. 7a). Similar changes have elsewhere been attributed to temporal changes in the electrical properties of the fault (Honkura et al., 1996) due to the upcoming earthquake. However, we observed similar changes in the polarization of electric fields between identical 25-day periods in 1997, when no large earthquakes (M>5) occurred in the area (Fig. 7b). In addition, the long-term magnetic field polarization over the same time periods show slight changes in direction around the time of the earthquake, but also show similar changes the year before (1997) when no earthquake occurred (data not shown).

3. Scaling calculations

Based on reports of previous ULF anomalies before $M \geq 6$ earthquakes and the lack of any obvious ULF precursor for this M_w 5.1 earthquake, we assume that electromagnetic precursors are related, inter alia, to the size of the earthquake. Because precursory magnetic fields are likely due to fluids in the fault zone (e.g., Draganov et al.,1991; Fenoglio et al., 1995; Merzer and Klemperer, 1997), we choose as an initial assumption that such fields are related to the volume of the earthquake rupture zone in which such fluids might exist and have participated in the earthquake preparation phase.

Based on this assumption, we can make an order of magnitude estimate of the amplitude of the magnetic anomaly expected prior to the M_w 5.1 SJB earthquake compared to the maximum anomaly of 5 nT observed in the 0.01–0.02 Hz band 3 h prior to the M_s 7.1 Loma Prieta earthquake (Fraser-Smith et al., 1993). (Note that Fig. 1 shows a maximum anomaly of 3 nT because the averaging of data took place over a period of days.) The seismic moment of an earthquake, M_o, is defined as

$$M_o = \mu \Delta \upsilon S \tag{1}$$

where μ is the shear modulus, $\Delta\upsilon$ is the slip on the fault plane, and S is the area of the fault plane (e.g., Udias, 1999). The stress drop of an earthquake is given by

$$\Delta\sigma = C\mu\Delta\upsilon/r \tag{2}$$

where C is a constant related to the shape of the fracture and r is the length dimension of the fault plane (e.g., Udias, 1999). Using Eqs. (1) and (2), we can solve for the stress drop in terms of the seismic moment:

$$\Delta\sigma = CM_o/rS. \tag{3}$$

The volume dimension of the rupture zone, V, can be roughly estimated as

$$V = (rS)^{2/3}x \tag{4}$$

where x represents the width of the fault zone. We can rewrite Eq. (4) in terms of the seismic moment and stress drop as

$$V \cong (CM_o/\Delta\sigma)^{2/3}x. \tag{5}$$

Next, we assume the same fracture-shape constant C and stress drop $\Delta\sigma$ [50 bars: Kanamori and Satake, 1996], for both the Loma Prieta (LP) and SJB earthquakes. The hypothesis that the stress drop is approximately constant for all earthquakes has been confirmed empirically by Aki (1972) and Kanamori and Anderson (1979). Hence

$$V \propto M_o^{2/3}x. \tag{6}$$

Because the width of the fault zone, x, of each earthquake is poorly determined from the respective aftershock distributions, we can assume that the volume dimension is directly proportional to M_o. Therefore, the ratio of the volume dimension of the LP earthquake to the volume dimension of the SJB earthquake, and consequently the ratio of magnetic anomalies prior to each of the earthquakes, is approximately equal to the ratio of their seismic moments. Using the appropriate seismic moments for the LP and SJB earthquakes of 3×10^{19} N m (Kanamori and Satake, 1996) and 5.32×10^{16} N m (Uhrhammer et al., 1999), respectively, the ratio of these moments, R, is approximately equal to 564.

Finally, we assume that the precursory magnetic field is generated at the hypocentral depth of the earthquake. The attenuation of electromagnetic fields produced by electric- or magnetic-dipole sources submerged in a conducting medium is characterized by the skin depth, δ, defined as

$$\delta = (\pi f \mu \sigma)^{-1/2} \tag{7}$$

where f is the frequency, μ is the permeability of the medium (we use the permeability of free space, μ_o, where $\mu_o = 4\pi \times 10^{-7}$ H/m), and σ is the electrical conductivity (Telford et al., 1990). This skin depth is the measure of distance over which the amplitude of the wave is attenuated to $1/e$ of its original value. Considering that the epicenters of both the LP and SJB earthquakes were within 7 km of the recording instruments, and that there is minimum attenuation of the electromagnetic waves when they propagate along the surface of the earth (Bubenik and Fraser-Smith, 1978), the magnetic field observed on the surface, H_{surf}, is

$$H_{surf} = H_{hyp}\, e^{-(d/\delta)} \tag{8}$$

where H_{hyp} is the magnetic field generated at the hypocenter and d is the hypocentral depth. We use Eqs. (7) and (8), the hypocentral depth of 17 km for the LP earthquake (Dietz and Ellsworth, 1990), the appropriate crustal conductivity of 0.01 S/m (Unsworth et al., 1997; M. Unsworth, personal communication), and a maximum surface anomaly of 5 nT to calculate a 7-nT field generated at the hypocenter of the LP earthquake. Assuming

$$H_{hyp\_SJB}/H_{hyp\_LP} = R, \quad (9)$$

we calculate H_{hyp} of the SJB earthquake to be 0.012 nT. Using Eq. (8) and the approximate hypocentral depth of 9.2 km for SJB (Uhrhammer et al., 1999), we calculate an expected magnetic anomaly measured at the surface prior to the SJB earthquake of $\sim$ 0.01 nT.

A 0.01-nT anomaly is on the order of the increase observed in the subtracted data shown in Fig. 5C, but of course 0.01 nT is less than the noise level measured at SAO (Fig. 5D). However, our observations are consistent with the hypothesis that any magnetic field anomaly scales with the volume of the earthquake rupture zone, and hence is related to the seismic moment.

4. Reexamination of previously proposed mechanisms

It is important to keep in mind that because of varying physical properties of faults, it is unlikely that similar precursory signals would be produced by all earthquakes. Nevertheless, we can use these physical properties along with our observations to constrain further the mechanism by which a ULF precursor may be produced and the dependence of that mechanism on the size of the earthquake. Although the 1989 Loma Prieta earthquake and the 1998 SJB earthquake occurred on two distinct fault zones, they are two strike-slip earthquakes that occurred within 50 km of each other in similar geological settings. Various mechanisms were proposed to explain the anomalous magnetic fields observed prior to the M 7.1 Loma Prieta earthquake. We reexamine four of these mechanisms in order to see whether they are likely also to explain our observations prior to the M 5.1 SJB earthquake, a smaller earthquake in a similar geological setting.

4.1. Dilatant-conductive effects

Merzer and Klemperer (1997) proposed that the anomalous fields observed prior to the 1989 Loma Prieta earthquake (Fig. 1) could have been due to the formation of a long, thin, highly conductive region along the fault, which magnified the external electromagnetic waves incident on the earth's surface. A precursory reorganization of the geometry of fluid-filled porosity in the fault-zone, termed the 'dilatant-conductive effect,' could produce such a high conductivity zone. According to this model, an elliptical conductor approximating the size of the fault zone, extending from the surface to the hypocenter (18 km deep) with a width of 4.5 km and a conductivity of 5 S/m, can produce the large magnetic field anomaly observed 3 h before the Loma Prieta main shock.

Based on this model, we estimated the magnetic field anomaly expected prior to the SJB earthquake assuming a 5 S/m conductivity zone extending from the surface to the hypocentral depth of $\sim$ 9 km and with a width of 500 m (width of aftershock zone). We calculated the expected anomaly at 0.01 Hz because this is the frequency at which the maximum Loma Prieta anomaly occurred, as well as the frequency at which we observe the largest 'increase' in ULF activity prior to the SJB earthquake (Fig. 5). We used a simplified two-layer conductivity model for the region outside of the fault zone that consists of a top layer 2.5-km thick with a conductivity of 0.1 S/m and a bottom layer (half-space) with a conductivity of 0.01 S/m (Unsworth et al., 2000). We also assumed a value of 1 A/m for the ambient magnetic field at the surface following the analysis carried out by Merzer and Klemperer (1997). The increase in magnetic field at 0.01 Hz expected prior to the SJB earthquake according to this dilatant-conductive model is $\sim$ 8 times that of background. Prior to the subtraction of data from the remote station PKD (Fig. 5), we observe a maximum increase in magnetic field activity of about 7–8 times background level (from $\sim$ 0.01 to $\sim$ 0.08 nT). However, once we subtract the contemporaneous data from PKD, we only see a twofold increase in the magnetic field (Fig. 6).

Considering that we calculated a maximum estimate of the magnetic field signal produced by the dilatant-conductive effect, it is possible that a signal may have been produced by this effect prior to the

SJB earthquake, but that it was too small to observe amongst the background noise. However, the magnetic field signal produced by this dilatant-conductive effect is extremely sensitive to the conductivity values assumed for both the high conductivity fault zones as well as the surrounding conductivity profile and to the geometry of the high conductivity zone. For example, if we assume that the high conductivity zone does not extend to the surface, a more likely scenario considering the rupture in the SJB earthquake did not break the surface, and rather that the conductivity zone extends more appropriately to the top of the aftershock zone (~ 4 km depth), then the maximum magnetic-signal produced would be approximately half the background noise level.

On the other hand, if we assume that there is a high conductivity zone that extends along the creeping segment of the San Andreas fault (the creeping segment extends approximately from stations SAO to PKD), then the dilatant-conductive effect could explain why we see enhanced signals at SAO and PKD, but not at station JSR, which is just as close to SAO as PKD but is located along a locked portion of the San Andreas Fault. Magnetotelluric and seismic reflection surveys at Parkfield, CA (near PKD) and in Hollister, CA (near SAO) show that the creeping segment of the San Andreas fault is characterized by a vertical zone of high conductivity that is absent in locked segments of the fault (Unsworth et al., 1999,2000). The occurrence of creep in a high conductivity zone as well as many examples of fluid changes associated with creep (Johnson et al., 1973; Mortenson et al., 1977; Lippincott et al., 1985; Roeloffs et al., 1989) is consistent with the suggestion that creep events are fluid-driven. In conclusion, the dilatant-conductive effect is dependent on the size of the earthquake, and it is likely that the anomalous fields produced by this effect, if any, are too small to observe amongst the background noise at the present recording stations.

4.2. Electrokinetic effects

Fenoglio et al. (1995) proposed that the anomalous Loma Prieta signals were caused by electrokinetic signals resulting from fluid flow through pressurized fault-zone compartments. Electrokinetic effects (Ishido and Mizutani, 1981; Johnston, 1997) are the electrical currents (and magnetic fields) generated by fluid flow through the crust in the presence of an electrified interface at the solid–liquid boundaries. In their model, Fenoglio et al. (1995) suggested that the rupture of seals between fault-zone compartments produce rapid pore-pressure changes and non-uniform fluid flow through newly formed fractures that propagate away from the high-pressure compartments. Assuming these fracture lengths are less than 200 m, the electrokinetic signals produced by this unsteady flow are comparable in magnitude and frequency to the magnetic signals observed prior to the Loma Prieta earthquake.

According to this fault-zone model, the variation in pressure across the fracture, from near-lithostatic at the rupture boundary to near-zero at the fracture tip, reduces the silica solubility, and silica deposition near the fracture tip decreases permeability reducing and perhaps stopping further fluid flow and fracture propagation. Pressure then builds in the fracture until rupture of the temporary seal occurs and the shear-fracture propagation continues. Each time a seal ruptures or a shear fractures stops and starts, fluid motion occurs, possibly generating observable magnetic field changes.

In order to obtain this non-uniform fluid flow, a variation in silica solubility across the fracture must accompany the variation in pressure across the fracture. At 17 km depth, the approximate depth at which the Loma Prieta earthquake occurred, the silica solubility across the fracture drops from 1 wt.% near the lithostatic high-pressure compartment to less than 0.5 wt.% at the fracture tip (Fenoglio et al., 1995, their Fig. 3). Consequently, it is likely that silica deposition near the fracture tip will decrease permeability and perhaps stop fluid flow. However, at 9 km depth, the approximate depth of the SJB earthquake, the difference between silica solubility across the fracture is less than 0.1 wt.% (Fenoglio et al., 1995; Fournier, 1995). It is unlikely that this difference is significant enough to cause more silica deposition at the fracture tip than at the rupture boundary, and, therefore, at this depth non-uniform fluid flow according to this model is unlikely. Consequently, for shallow (<15 km depth) earthquakes, the Fenoglio et al. mechanism is unlikely to produce precursory magnetic and electric fields.

In addition, according to the analysis of Fenoglio et al., the electrokinetic signals produced are depend-

ent on the geometry of the fractures produced, but not on the size of the earthquake. Furthermore, the frequency of the signal produced is inversely proportional to the fracture length. The physical parameters used in Fenoglio's analysis, such as porosity, fracture permeability, and density of rock, would likely be similar for both the Loma Prieta and SJB earthquakes. In this case, if this mechanism is truly independent of the size of the earthquake, then we should expect to see similar magnetic field anomalies prior to the SJB earthquake that were observed prior to the Loma Prieta earthquake. This is clearly not the case. If, on the other hand, we assume that the size of the fracture also relates to the size of the earthquake, then fractures produced prior to the SJB earthquake would be smaller than those produced prior to the Loma Prieta earthquake. However, in this case, magnetic signals would also peak at higher frequencies. If we assume a fracture length of 50 m (as opposed to 200 m assumed by Fenoglio et al., 1995), then we would expect to see a maximum magnetic field anomaly at ~ 0.2 Hz. The magnetic field increase that we observed prior to the SJB earthquake peaked at 0.01 Hz, and we did not observe any such increase at higher frequencies. It is therefore unlikely that an electrokinetic mechanism based on the fault-zone model proposed by Fenoglio et al. (1995) can explain our electric and magnetic field observations prior to the SJB earthquake.

4.3. Magnetohydrodynamic effects

The induced magnetic field, B_i, generated by the motion of a conductive fluid, referred to as the magnetohydrodynamic (MHD) effect, is strongly governed by the flow velocities and fluid electrical conductivities in the crust. The MHD effect can be approximated by

$$B_i = \mu\sigma v d B_o \quad (10)$$

where v is the flow velocity, d is the length scale of the flow, and B_o is the external magnetic field. Fluid flow in fractured fault zones at seismogenic depths ($\sim$ 5km) with a length scale of 1 km could generate transient fields of about 0.01 nT, assuming flow velocities less than a few mm/s and fluid conductivities no greater than that of seawater ($\sim$ 1 S/m) (Johnston, 1997). Draganov et al. (1991) proposed an MHD model for the region surrounding the Loma Prieta earthquake in which they calculated surface magnetic fields of ~ 0.1 nT. However, the very high flow velocity ($\sim$ 4 cm/s) required by their model requires an unrealistically high permeability value on the order of 10^{-10} m^2. Furthermore, if they assumed a more realistic permeability on the order of 10^{-11} m^2, the pore pressures needed to obtain an $\sim$ 4 cm/s fluid flow would be 40 GPa, two orders of magnitude greater than lithostatic (about 400 MPa at 4 km depth) (Fenoglio et al., 1995).

A rough estimate of the magnetic field produced by the MHD effect prior to the SJB earthquake would assume a minimum permeability of 10^{-11} m^2, a pore pressure gradient of 4×10^4 Pa/m, and consequently a velocity of $\sim$ 4 mm/s. In this case, a length scale of 1 km could generate transient fields of about ~ 0.2 nT. This is over twice as large as the fields we observed a few hours prior to the SJB earthquake, and it is definitely within the sensitivity range of our equipment. If our suggested scaling applies, then either the permeability of, and fluid flow within, the San Andreas Fault differ considerably from Loma Prieta to San Juan Bautista, or the MHD effect was not the cause of the Loma Prieta precursor. Without more information regarding the permeability and conductivity of the fault zone it is difficult to speculate about MHD-induced fields.

4.4. Piezomagnetic effects

Piezomagnetic effects result from a change in magnetization of ferromagnetic-bearing rock in response to applied stress. Piezomagnetic anomalies of a few nT should be expected to accompany earthquakes (Johnston, 1997), but it is likely that piezomagnetic effects prior to earthquakes are too small to observe. We do not observe any potential piezomagnetic signals (> 0.1 nT) at the occurrence time of the SJB earthquake (see Fig. 3). Fenoglio et al. (1995) calculated a maximum magnetic field of 0.01 nT produced by piezomagnetic effects in the surrounding rock due to high pore pressures acting along the walls of shear fractures prior to the Loma Prieta earthquake. Assuming a similar model, these effects are too small or only contribute partly to the observed fields prior to the SJB earthquake.

5. Conclusion

Based on the dilatant-conductive effect and the piezomagnetic effect, if anomalous precursory magnetic and/or electric fields were produced prior to the SJB earthquake, it is unlikely that they could be observed above the background noise at the current ULF stations. On the other hand, the electrokinetic model proposed by Fenoglio et al. (1995) and the MHD effect do not predict results consistent with our observations, though it is difficult to correctly apply these mechanisms without further information regarding the physical properties and geometry of the fault zone.

Exploring and constraining various mechanisms such as those discussed above is an important next step in understanding electromagnetic signals associated with earthquakes. However, the most immediate need in earthquake-related EM studies is a database of good measurements with multiple instruments during moderately large and large earthquakes. Such measurements will constrain the possible relationship between EM signals and earthquakes and their possible generation mechanisms.

In conclusion, because EM stations cannot be significantly quieter, we need to focus on earthquakes with $M>6$. It may at present be impossible to test whether earthquakes with $M \leq 5$ have associated magnetic anomalies of the Loma Prieta type.

Acknowledgements

We thank the Northern California Earthquake Data Center (NCEDC) and Dr. H.F. Morrison, Sierra Boyd, and colleagues at the Seismological Laboratory at UC Berkeley for use of data from the EM station SAO. We thank Greg Beroza and Norm Sleep for their constructive reviews and helpful discussions. In addition, we greatly appreciate Moshe Merzer's guidance and discussion regarding the calculations involved with the dilatant-conductive effect.

References

Aki, K., 1972. Earthquake mechanism. Tectonophysics 13, 423–446.

Bernardi, A., Fraser-Smith, A.C., Villard Jr., O.G., 1989. Measurements of BART magnetic fields with an automatic geomagnetic pulsation index generator. IEEE Trans. Electromagn. Compat. 31, 413–417.

Bernardi, A., Fraser-Smith, A.C., McGill, P.R., Villard Jr., O.G., 1991. Magnetic field measurements near the epicenter of the M_s 7.1 Loma Prieta earthquake. Phys. Earth Planet. Inter. 68, 45–63.

Bubenik, D.M., Fraser-Smith, A.C., 1978. ULF/ELF electromagnetic fields generated in a sea of finite depth by a submerged vertically-directed harmonic magnetic dipole. Radio Sci. 13, 1011–1020.

Dietz, L.K., Ellsworth, W.L., 1990. The October 17, 1989, Loma Prieta, California, earthquake and its aftershocks; geometry of the sequence from high-resolution locations. Geophys. Res. Lett. 17, 1417–1420.

Draganov, A.B., Inan, U.S., Taranenko, Y.N., 1991. ULF magnetic signatures at the earth due to groundwater flow: a possible precursor to earthquakes. Geophys. Res. Lett. 18, 1127–1130.

Fenoglio, M.A., Fraser-Smith, A.C., Beroza, G.C., Johnston, M.J.S., 1993. Comparison of ultra-low frequency electromagnetic signals with aftershock activity during the 1989 Loma Prieta earthquake sequence. Bull. Seismol. Soc. Am. 83, 347–357.

Fenoglio, M.A., Johnston, M.J.S., Byerlee, J.D., 1995. Magnetic and electric fields associated with changes in high pore pressure in fault zones: application to the Loma Prieta ULF emissions. J. Geophys. Res. 100, 12951–12958.

Fournier, R.O., 1995. Continental scientific drilling to investigate brine evolution and fluid circulation in active hydrothermal systems. In: Raleigh, C.B. (Ed.), Observations of the Continental Crust Through Drilling I. Springer, Berlin, pp. 98–122.

Fraser-Smith, A.C., Bernardi, A., McGill, P.R., Ladd, M.E., Helliwell, R.A., Villard Jr., O.G., 1990. Low-frequency magnetic measurements near the epicenter of the M_s 7.1 Loma Prieta earthquake. Geophys. Res. Lett. 17, 1465–1468.

Fraser-Smith, A.C., Bernardi, A., Helliwell, R.A., McGill, P.R., Villard, O.G., 1993. Analysis of low frequency electromagnetic field measurements near the epicenter of the M_s 7.1 Loma Prieta, California, earthquake of October 17, 1989. In: Johnston, M.J.S. (Ed.), Preseismic Observations. U.S. Geol. Surv. Prof. Pap., vol. 1550-C. U.S. Geological Survey, Reston, VA, C17–C25.

Gershenzon, N.I., Bambakidis, G., 2001. Modeling of seismo-electromagnetic phenomena. Rus. J. Earth Sci. 3, 247–275.

Gershenzon, N.I., Gokhberg, M.B., 1994. On the origin of anomalous ultra-low frequency geomagnetic disturbances prior to the Loma Prieta, California, earthquake. Phys. Solid Earth 30, 112–118.

Haartsen, M.W., Pride, S.R., 1997. Electroseismic waves from point sources in layered media. J. Geophys. Res. 102, 24745–24769.

Hayakawa, M., Kawate, R., Molchanov, O.A., Yumoto, K., 1996. Results of ultra-low-frequency magnetic field measurements during the Guam earthquake of 8 August 1993. Geophys. Res. Lett. 23, 241–244.

Honkura, Y., Tsunakawa, H., Matsushima, M., 1996. Variations of the electric potential in the vicinity of the Nojima fault during the activity of aftershocks of the 1995 Hyogo-ken Nanbu earthquake. J. Phys. Earth 44, 397–403.

Ishido, T., Mizutani, H., 1981. Experimental and theoretical basis of electrokinetic phenomena in rock-water systems and its application to geophysics. J. Geophys. Res. 86, 1763–1775.

Johnson, A.G., Kovach, R.L., Nur, A., 1973. Pore pressure changes during creep events on the San Andreas Fault. J. Geophys. Res. 78, 851–857.

Johnston, M.J.S., 1997. Review of electric and magnetic fields accompanying seismic and volcanic activity. Surv. Geophys. 18, 441–475.

Kanamori, H., Anderson, D.L., 1979. Theoretical basis of some empirical relations in seismology. Bull. Seismol. Soc. Am. 65, 1073–1095.

Kanamori, H., Satake, K., 1996. Broadband study of the source characteristics of the earthquake. In: Spudich, P. (Ed.), The Loma Prieta, California, earthquake of October 17, 1989—mainshock characteristics. U.S. Geol. Surv. Prof. Pap., vol. 1550-A. U.S. Geological Survey, Reston, VA, A75–A80.

Karakelian, D., Klemperer, S.L., Fraser-Smith, A.C., Beroza, G.C., 2000. A transportable system for monitoring ultra-low frequency electromagnetic signals associated with earthquakes. Seismol. Res. Lett. 71, 423–436.

Karakelian, D., Beroza, G.C., Klemperer, S.L., Fraser-Smith, A.C. (in press). Analysis of ultra-low frequency electromagnetic field measurements associated with the 1999 M 7.1 Hector Mine earthquake sequence, Bull. Seismol. Soc. Am.

Kopytenko, Y.A., Matiashvili, T.G., Voronov, P.M., Kopytenko, E.A., Molchanov, O.A., 1993. Detection of ultra-low frequency emissions connected with the Spitak earthquake and its aftershock activity, based on geomagnetic pulsations data at Dusheti and Vardzia observatories. Phys. Earth Planet. Inter. 77, 85–95.

Kopytenko, Y.A., Ismaguilov, V.S., Kopytenko, E.A., Molchanov, O.A., Voronov, P.M., Hattori, K., Hayakawa, M., Zaitzev, D.B. (submitted for publication). Magnetic phenomena in ULF range connected with seismic sources, Ann. Geophys.

Lippincott, D.K., Bredehoeft, J.D., Moyle Jr., W.R., 1985. Recent movements on the Garlock fault as suggested by water-level fluctuations in a well in Fremont Valley, California. J. Geophys. Res. 90, 1911–1924.

Merzer, M., Klemperer, S.L., 1997. Modeling low-frequency magnetic-field precursors to the Loma Prieta earthquake with a precursory increase in fault-zone conductivity. Pure Appl. Geophys. 150, 217–248.

Molchanov, O.A., Kopytenko, Yu.A., Voronov, P.M., Kopytenko, E.A., Matiashvili, T.G., Fraser-Smith, A.C., Bernardi, A., 1992. Results of ULF Magnetic field measurements near the epicenters of the Spitak (M_s = 6.9) and Loma Prieta (M_s = 7.1) earthquakes: comparative analysis. Geophys. Res. Lett. 19, 1495–1498.

Mortenson, C.E., Lee, R.C., Burford, R.O., 1977. Observations of creep related tilt, strain, and water level changes on the central San Andreas fault. Bull. Seismol. Soc. Am. 67, 641–649.

Nagao, T., Orihara, Y., Yamaguchi, T., Takahashi, I., Hattori, K., Noda, Y., Sayanagi, K., Uyeda, S., 2000. Co-seismic geoelectric potential changes observed in Japan. Geophys. Res. Lett. 27, 1535–1538.

Park, S.K., Johnston, M.J.S., Madden, T.R., Morgan, F.D., Morrison, H.F., 1993. Electromagnetic precursors to earthquakes in the ULF band: a review of observations and mechanisms. Rev. Geophys. 31, 117–132.

Peltzer, G., Rosen, P., Rogez, F., Hudnut, K., 1996. Postseismic rebound in fault step-overs caused by pore fluid flow. Science 273, 1202–1204.

Roeloffs, E.A., Burford, S.S., Riley, F.S., Records, A.W., 1989. Hydrologic effects on water level changes associated with episodic fault creep near Parkfield, California. J. Geophys. Res. 94, 12387–12402.

Telford, W.M., Geldart, L.P., Sheriff, R.E., 1990. Applied Geophysics, 2nd ed. Cambridge Univ. Press, New York, 770 pp.

Udias, A., 1999. Principles of Seismology Cambridge Univ. Press, New York, 475 pp.

Uhrhammer, R.A., Karavas, W., Romanowicz, B., 1998. Broadband seismic station installation guidelines. Seismol. Res. Lett. 69, 15–26.

Uhrhammer, R., Gee, L.S., Murray, M., Dreger, D., Romanowicz, B., 1999. The *Mw* 5.1 San Juan Bautista, California Earthquake of 12 August 1998. Seismol. Res. Lett. 70, 10–18.

Unsworth, M.J., Malin, P.E., Egbert, G.D., Booker, J.R., 1997. Internal structure of the San Andreas fault at Parkfield, California. Geology 25, 359–362.

Unsworth, M., Egbert, G., Booker, J.R., 1999. High-resolution electromagnetic imaging of the San Andreas Fault in Central California. J. Geophys. Res. 104, 1131–1150.

Unsworth, M.J., Bedrosian, P.A., Egbert, G.D., 2000. Correlation of electrical structure and seismicity along the San Andreas Fault in central California. EOS, Transactions, AGU 81, F1214.

Villante, U., Vellante, M., Piancatelli, A., 2001. Ultra low frequency geomagnetic field measurements during earthquake activity in Italy (September–October 1997). Ann. Geophys. 44, 229–237.

Zanzerkia, E.E., Beroza, G.C., 2001. Pore fluid effects on nucleation of aftershocks of the Landers earthquake, SSA 2001 Meeting Abstract. Seismol. Res. Lett. 72, 263.

Zlotnicki, J., Kossobokov, V., Le Mouël, J., 2001. Frequency spectral properties of an ULF electromagnetic signal around the 21 July 1995, M = 5.7, Yong Deng (China) earthquake. Tectonophysics 334, 259–270.